JWMM

Numerical Simulation of Flood Propagation in the Kelara River Flood Early Warning System

Farouk Maricar, Riswal Karamma, Muhammad Rifaldi Mustamin and Muhammad Farid Maricar (2023)
Hasanuddin University, Indonesia

DOI: https://doi.org/10.14796/JWMM.C501

ABSTRACT

Flood historical data from the Kelara River in the last 10 years shows that the river has often overflowed, and the worst floods happened on January 22, 2019. One of the efforts to minimize the negative impact of a flood disaster is to conduct flood tracking. Flood tracking is an analysis of the flood along the river, or also known as flood propagation, which can be used as a reference in the preparation of a flood early warning system. This study aims to determine the propagation of the Kelara River flood which can be used to determine flood-prone areas and as a reference in the preparation of a flood early warning system. This research was carried out in 3 stages, namely flood hydrology analysis using the HEC-HMS program, numerical simulation of 2D floods using the HEC-RAS program, spatial modeling of flood-prone areas using the ArcGIS program, and preparation of a flood early warning system. The results of this study showed that the flood that occurred on January 22, 2019, was a 100-year return period flood, and determined that 10 points of residential areas/villages must be alerted when the intensity of rain is high, with the fastest time to be alerted being 52 minutes.

1. INTRODUCTION

Among all natural disasters, flooding is the most frequent phenomenon and affects a large proportion of the population worldwide almost every year (Mujumdar 2001). In addition to the most frequent disasters, floods also have a wide scope and can cause great losses, including loss of life and property loss (Hallegatte et al. 2013; Merz et al. 2010; Wijayanti et al. 2017). Floods in

Maricar, F., R. Karamma, M.R. Mustamin, and M.F. Maricar. 2023. "Numerical Simulation of Flood Propagation in the Kelara River Flood Early Warning System." *Journal of Water Management Modeling* 31: C501. https://doi.org/10.14796/JWMM.C501 www.chijournal.org ISSN: 2292 6062

Indonesia have enormous potential when viewed from the topography which is mostly lowlands, basins, and oceans, and is also one of the countries that has extreme rainfall (Bakri et al. 2021).

Land clearing is also an important flooding factor because it changes catchment area conditions and surface runoff quantity. One of the watersheds that experienced a lot of land conversion from forest to residential and agricultural land (especially rice fields) is the Kelara watershed (Samsuar and Sapsal 2018). This is in line with research in the upstream Kelara watershed, which shows that there is a tendency to increase the value of the surface runoff coefficient (C) in 2009 by 0.166 and in 2018 by 0.173 increasing in flood discharge by 7-8% (Riswal and Sukri 2020).

According to historical flood data from the National Disaster Management Agency through the Indonesian Disaster Information Data (DIBI) website, there have been floods in Jeneponto Regency, more precisely on the Kelara River in 2010, 2015, 2018, 2019, 2020, and 2021. The worst floods occurred on January 22, 2019, when Jeneponto Regency was hit by floods with a height range of 50-600 cm. There were 11 sub-districts flooded with 15 people dead, 1 person missing, 937 houses damaged and 48 public facilities damaged with an average rainfall intensity of 107.7 mm. (Daftar Informasi Bencana Indonesia (DIBI) 2021). Problems caused by floods are increasing from year to year, therefore, it is important to get attention and efforts to overcome them properly (Satriani et al. 2021).

One of the steps in flood mitigation efforts is to conduct flood i tracking. Flood tracking is a way to determine the time and flood discharge (flood hydrograph) at a point in the flow based on the known upstream hydrograph. Flood tracking can also be interpreted as an analysis of the course of flooding along the river or also known as flood propagation. It is very important to study flood propagation in flood-prone areas which can later be used as a reference for flood early warning systems to anticipate and reduce losses from flood disasters (Sudarmin et al. 2022; Hou et al. 2020; Romali 2018; Lopa et al. 2018; Contreras et al. 2018; Xia et al. 2017; Di Baldassare et al. 2009).

The main component of a flood early warning system is numerical modeling, which is used for flood prediction (Yang et al. 2021; Vijayan et al. 2021; Praveen et al. 2020; Son and Jeong 2019; Krzhizhanovskaya et al. 2011). Numerical modeling is the answer to the limitations of the physical model, the limitations of direct observation, and the limitations of field measurement data. With the rapid advances in technology, currently the model has been developed and can be applied to flood simulations to determine flood arrival time, inundated area, water level, and flood flow velocity (Hou et al. 2021, 2018; Rak et al. 2016; Liang 2010).

Therefore, numerical models can play an important role in flood event prediction and evaluation of potential scenarios. Numerical models are now an important tool for understanding the spread and consequences of floods, planning future adaptations of cities affected by natural hazards, and developing early warning systems in urban areas.

In this paper, we introduce a numerical model for flood propagation along the river channel as a modeling of flood-prone areas that are urgently needed by the government in supporting infrastructure planning, transportation facilities, planning an area by developers to determine flood insurance and guarantees for buildings, houses, office buildings and provide an assessment of the time of flood propagation as a flood early warning system in anticipating the time and occurrence of the flood itself.

2. METHODOLOGY

This research was conducted in the Kelara River, Jeneponto Regency, South Sulawesi Province, Indonesia, which has a high potential for flooding based on historical flood events. This study was conducted in the middle stream area towards the downstream (estuary) along ± 35 km which is geographically located at 3°52'49. 82"LS and 120°0'32.07"E to 3°56'18. 85"LS and 119°57 '29.81"BT. For more details, the research location can be seen in Figure 1.

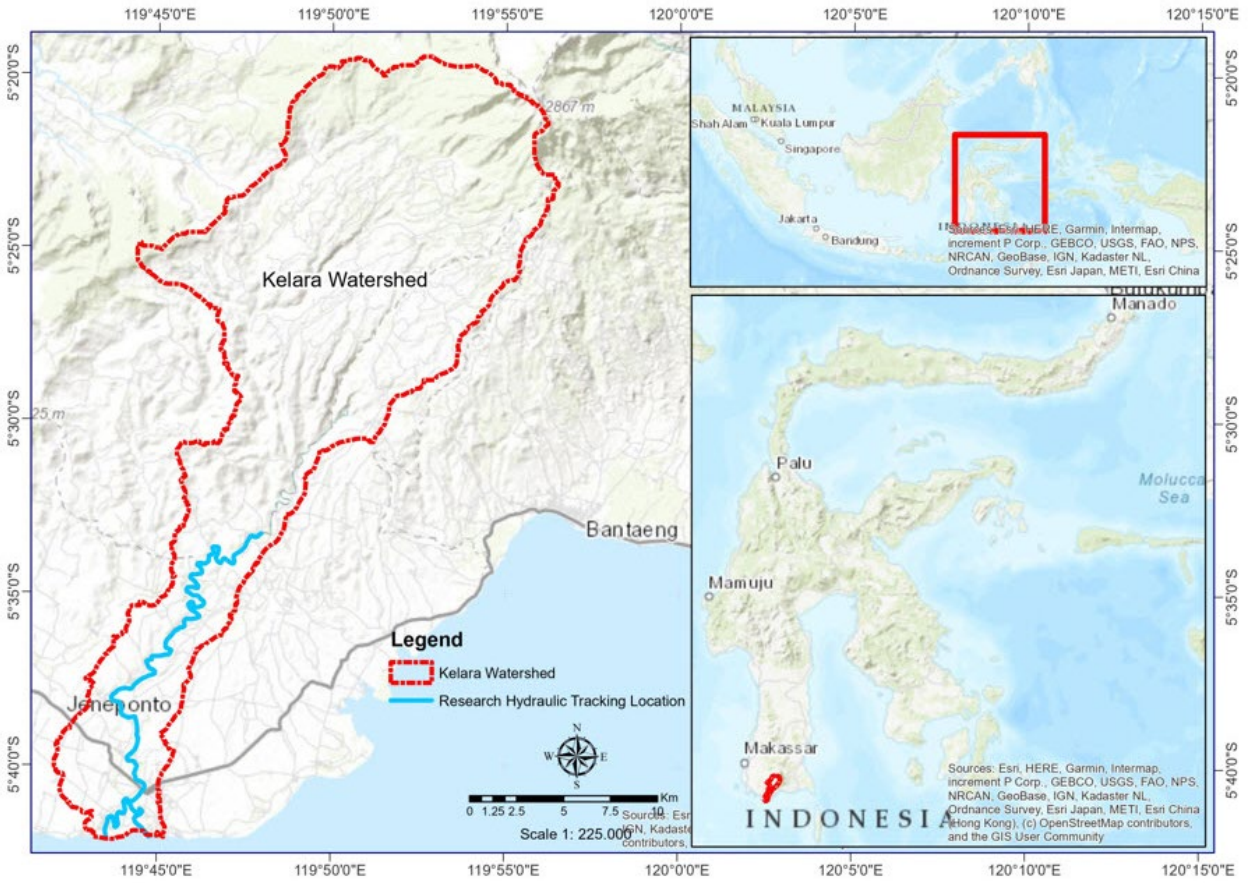

Figure 1 Study area location.

The concept of simulation modeling carried out in the research area uses 2D numerical simulations that can describe the flow profile in the river starting from hydrological calculations, hydraulic calculations, and inundation area calculations. This modeling includes hydrological modeling of watersheds and modeling of flood propagation areas in rivers and in inundation areas, which will later be used as a reference in the preparation of a flood early warning system.

2.1 Watershed flood hydrology modeling

Watershed hydrological modeling is intended to transform rainfall data to runoff. To find out the most appropriate method used in calculating flood discharge, it is necessary to compare the results of the analysis of several methods with the flood discharge results from field observations (Karamma and Pallu 2018). However, based on previous studies, hydrological modeling in the Kelara watershed shows that the HSS SCS method (HEC-HMS Application) is

closest to the Automated Water Level Recorder (AWLR) discharge and Crager Graph (Mustamin et al. 2021). In the hydrological analysis using the HEC-HMS application, the data used included land use data, soil type data, river topography, and TRMM (Tropical Rainfall Measuring Mission) rainfall data. Research related to the accuracy of TRMM has been investigated and shows that TRMM data has good performance in the Indonesian region and has a correlation with daily rainfall observation data, an average of 0.90 of the satellite rainfall data (Vernimmen et al. 2012). The detailed hydrological analysis stages can be seen in Figure 2.

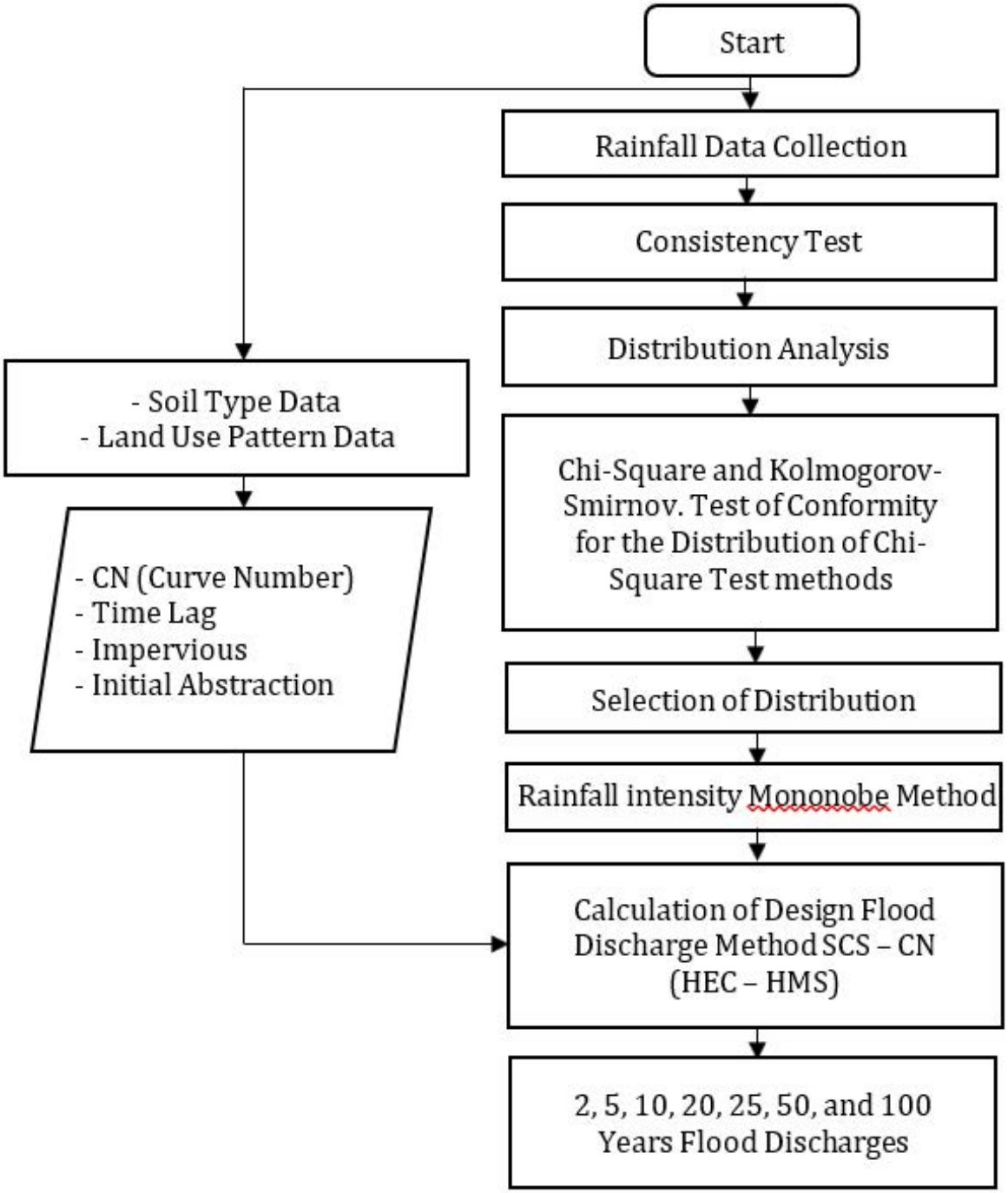

Figure 2 Flood analysis stages using the SCS-CN Method (HEC-HMS).

2.2 2D Numerical simulation

In performing a 2D HEC-RAS numerical simulation with an unsteady flow type, two equations can be used, namely Full Saint Vennant/Full Momentum and Diffusion Wave (Brunner 2016). In the simulation, the Diffusion Wave is used so that the simulation runs stably because the simulation area is wide in scope (Bagheri et al. 2020). Besides, it should be noted that the equations used in the computation of the 2D HEC-RAS model are the equations for quantity and momentum in the x & y-direction. Compiling a simulation model with the HEC-RAS application using the RAS Mapper tool, requires 3 input components, namely Terrain (to model the study field), Geometries (to describe the flow area model), and Land Cover (to input the Manning coefficient value).

The input to the terrain component is a combination of data from river topography and Digital Elevation Model National (DEMNAS) measurements with a spatial resolution of 8.4 m (0.27 arcSecond). The combination of the two is carried out to maximize the performance of the simulation considering that the resolution of DEMNAS is not yet able to read the existing river network. The detailed stages in the preparation of the terrain model can be seen in Figure 3.

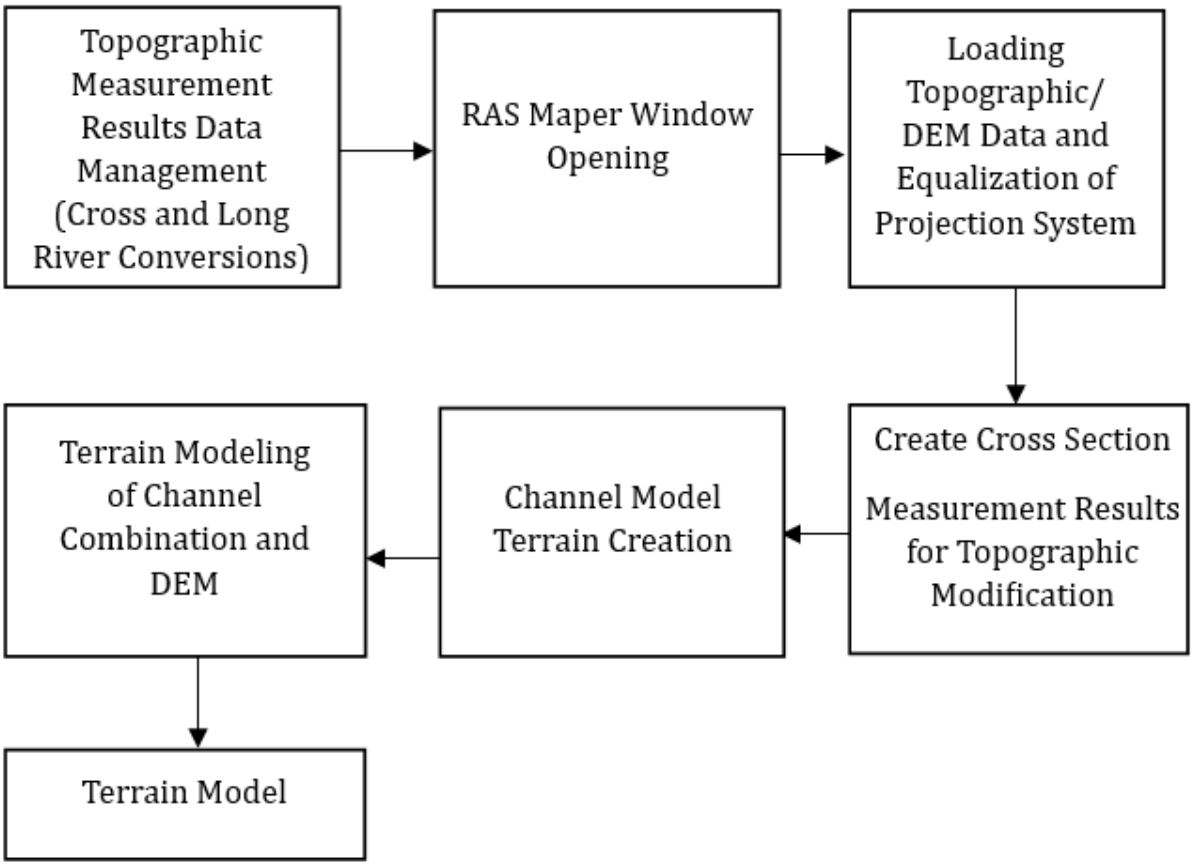

Figure 3 Terrain model preparation stages.

The geometric component is useful for describing the flow area model, which is the object of the simulation, where there are 3 inputs in the geometric component, namely 2D flow areas, break lines, and boundary conditions.

The 2D flow areas element functions to set and limit the area to be simulated with several

parameters. The break line on the river serves to reduce the grid size in the riverbed area so that it can increase accuracy in the simulation, reduce leaks in the 2D flow area, and errors during the simulation process. Furthermore, the boundary conditions element serves to determine the inflow and outflow points of the simulation. Inflow and outflow data are entered in the unsteady flow data menu, where inflow data in this study is based on the results of flood hydrology analysis.

The land cover component *b* is carried out by inputting spatial data on the manning value in the study field, where the Manning value refers to the Natural Resources Conservation Service (NRCS) based on land use patterns (Brunner 2016).

Overall, the stage details for preparing the 2D non-permanent flow simulation model consisting of terrain, geometries, and land cover that will be used for the simulation can be seen in Figure 4, and the results of the modeling can be seen in Figure 5.

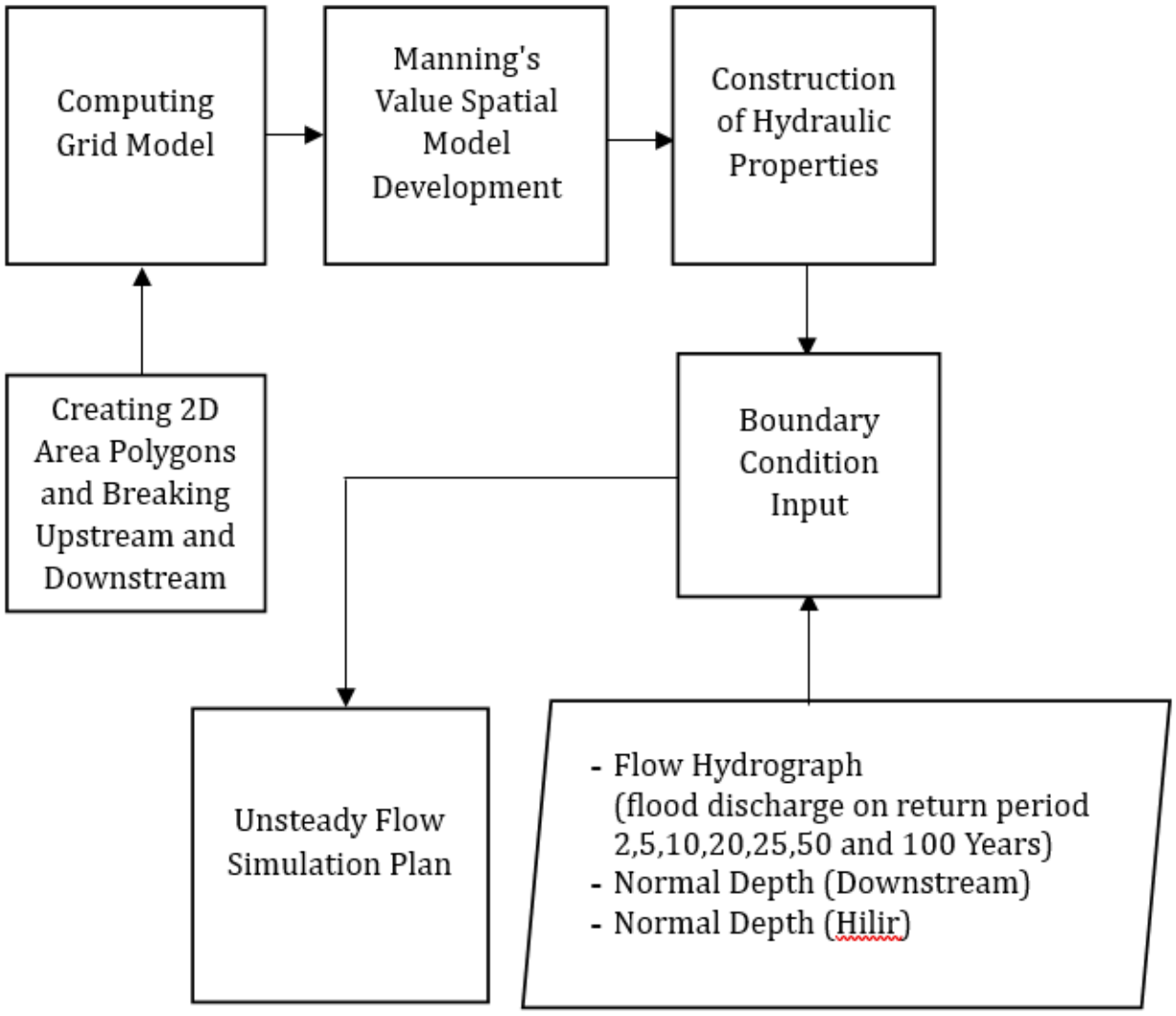

Figure 4 2D simulation model development stages.

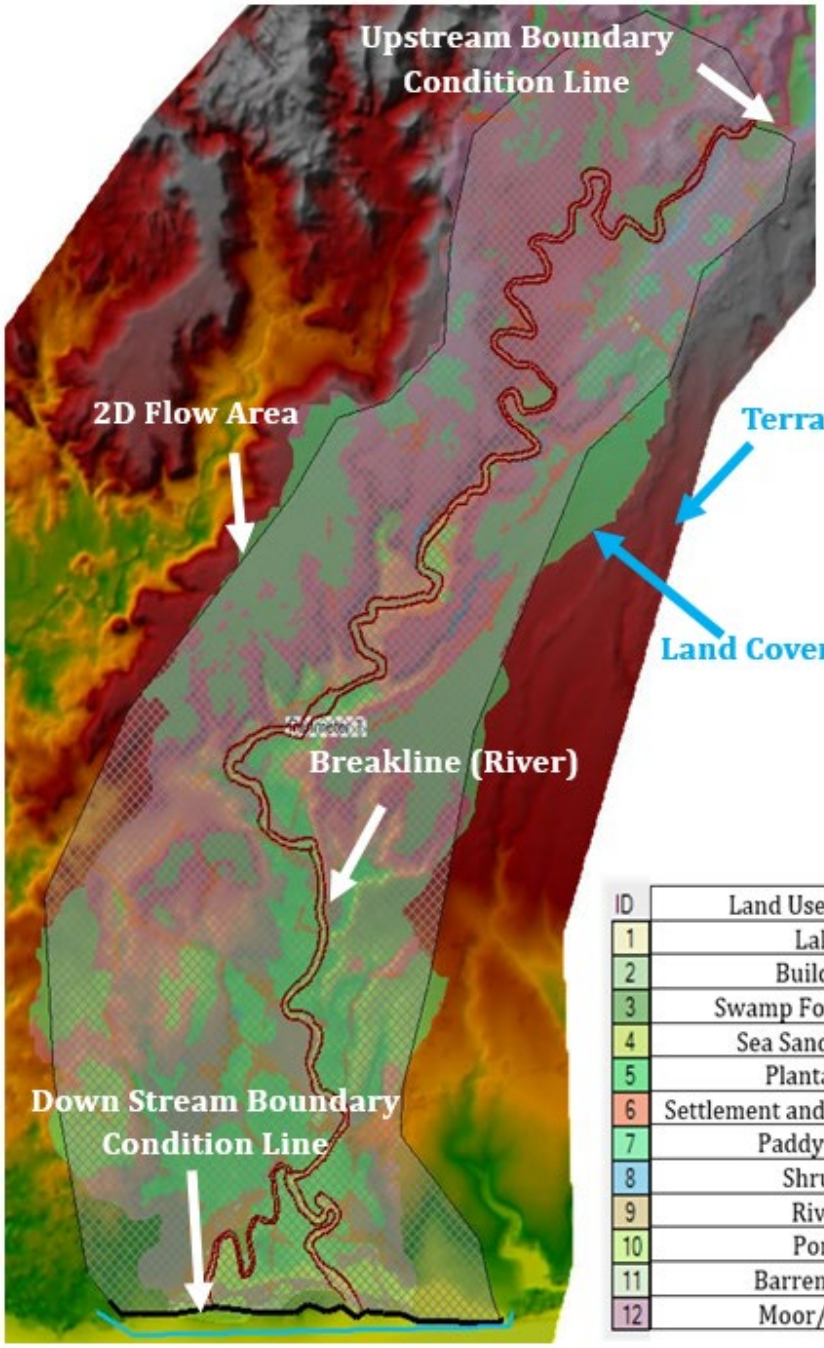

ID	Land Use Pattern	Mannings (N)
1	Lake	0.035
2	Building	0.015
3	Swamp Forest/Peat	0.12
4	Sea Sand Dunes	0.04
5	Plantation	0.06
6	Settlement and Activity Place	0.15
7	Paddy Field	0.06
8	Shrubs	0.08
9	River	0.035
10	Pond	0.04
11	Barren Land	0.04
12	Moor/Fleld	0.06

Figure 5 Elements in the HEC-RAS flood simulation.

From the simulation results, it will be seen that the flood propagation in the affected area is then mapped using the ArcGIS application as reference material for the flood early warning system.

2.3 Flood early warning system

If the flood-affected areas are known from the modeling, then the next step to minimize the impact of flooding on the Kelara River is to plan a flood early warning system by conducting a flood time travel analysis and an analysis of the critical time of lookout points. SE Director General of Natural Resources No. 05/SE/D/2016 concerning “Guidelines for the Implementation

of River Operations and Maintenance Activities" contains guidelines for flood alert levels. The determination of the standby level is divided into 3, namely green alert (1.2–1.5 m from freeboard), yellow alert (0.8–1.2 m from freeboard), and red alert (< 0.80 m from freeboard) (Modul Pengendalian Daya Rusak Air 2017). A general description of lookout points and flood alert levels can be seen in Figure 6.

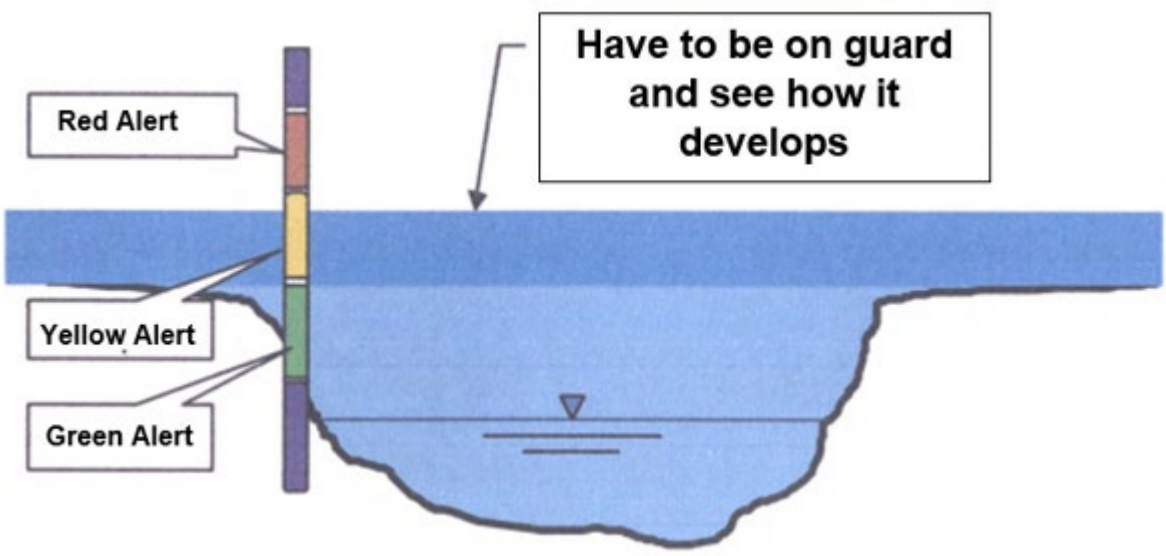

Figure 6 Flood lookout point.

The flood warning lookout points are placed at the point of occurrence of flood overflows and densely populated/populated areas, including flood-prone areas. In the flood early warning system, it is necessary to analyze the flood time travel from the simulation results to be able to estimate the total time from the upstream lookout point to the downstream lookout point to provide information on flood time travel/time travel, which aims to improve community preparedness in the event of extreme rain conditions.

To clarify, the stages, starting from the beginning of research activities, data collection, flood hydrology modeling, 2D numerical simulation to flood early warning systems, are illustrated in a flow chart which can be seen in Figure 7.

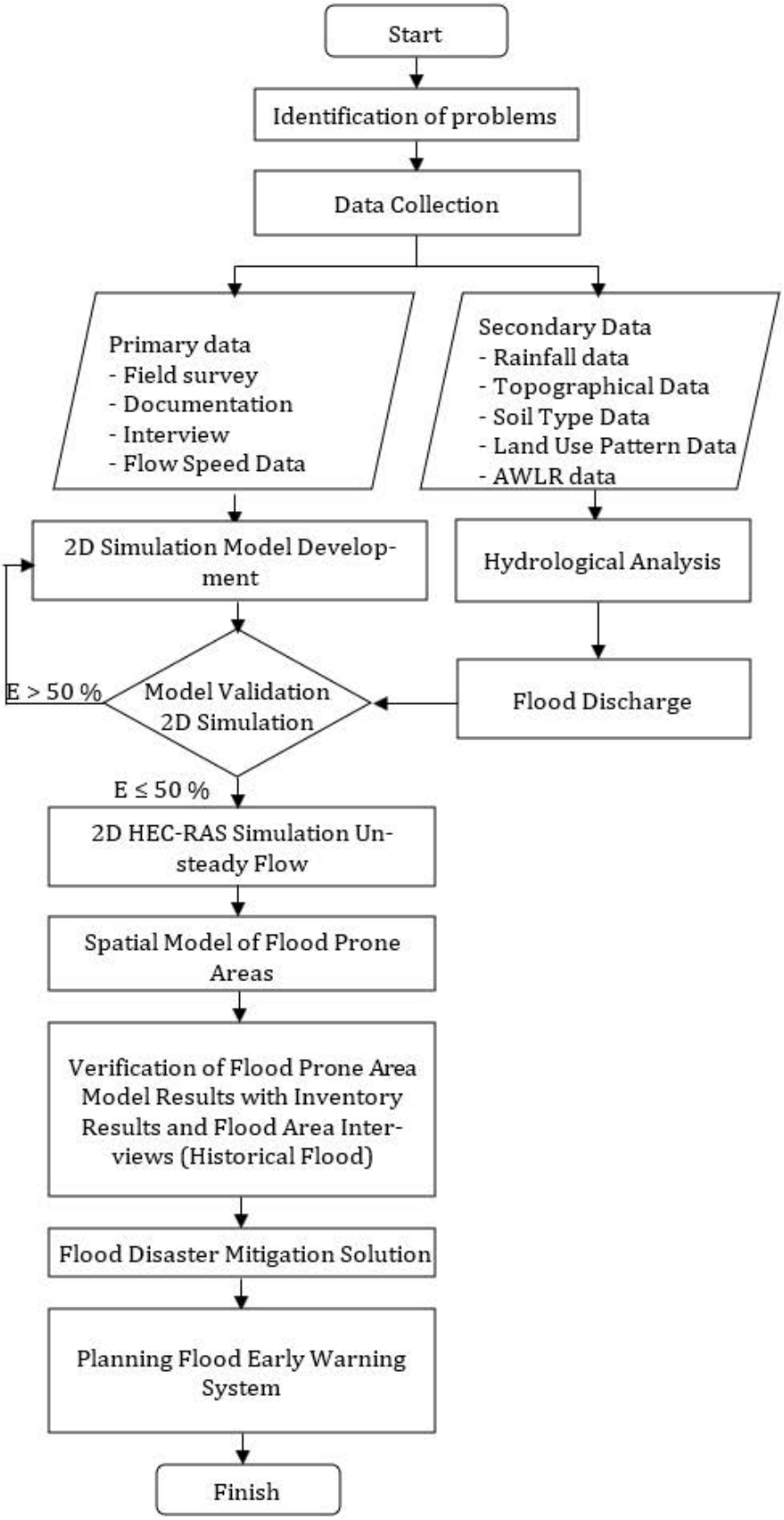

Figure 7 Research flowchart.

3. RESULTS AND DISCUSSION

3.1 Kelara Watershed flood hydrology

In hydrological analysis, the SCS method (HEC-HMS application) requires data input in the form of watershed characteristics such as topography, land use, and soil types that greatly affect rainwater, which will become runoff/runoff. The analysis of watershed characteristics using the ArcGIS application is very necessary, where spatial data from various agencies is processed intoa map to make it easier to analyze the characteristics of the watershed. In addition, this hydrological analysis also takes into account the reduction of flood discharge from the Karalloe Dam, which was built in the Karalloe sub-watershed. The following is a map that can be used to describe the characteristics of the Kelara watershed, which can be seen in Figure 8.

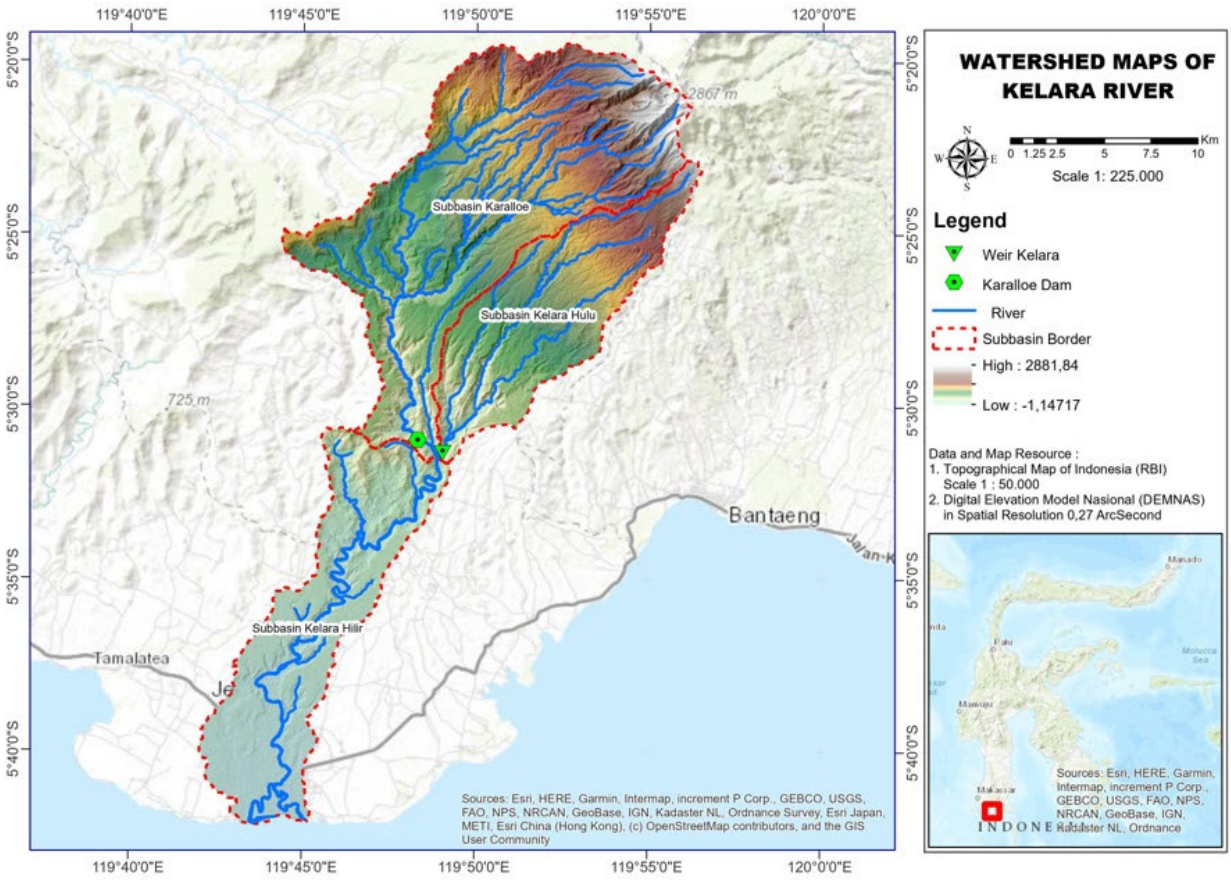

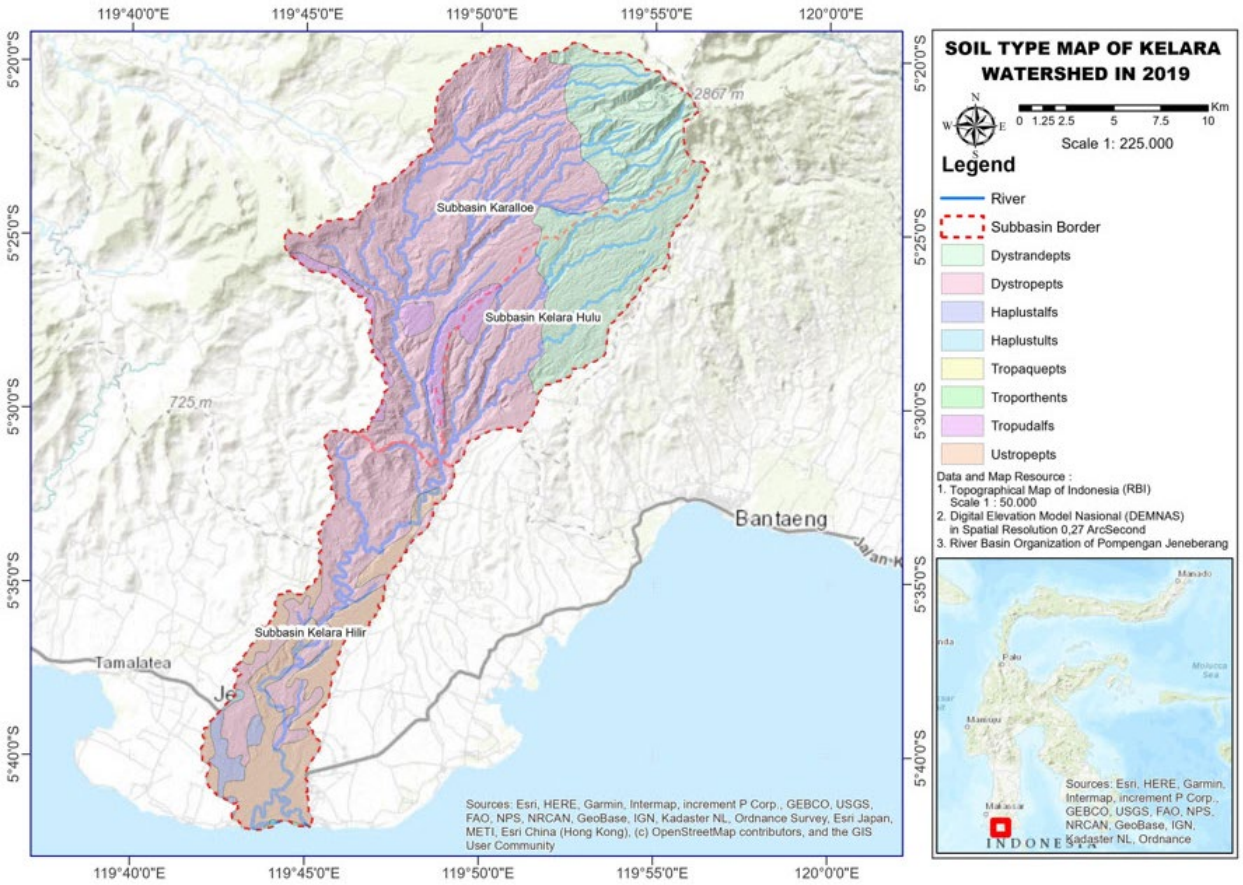

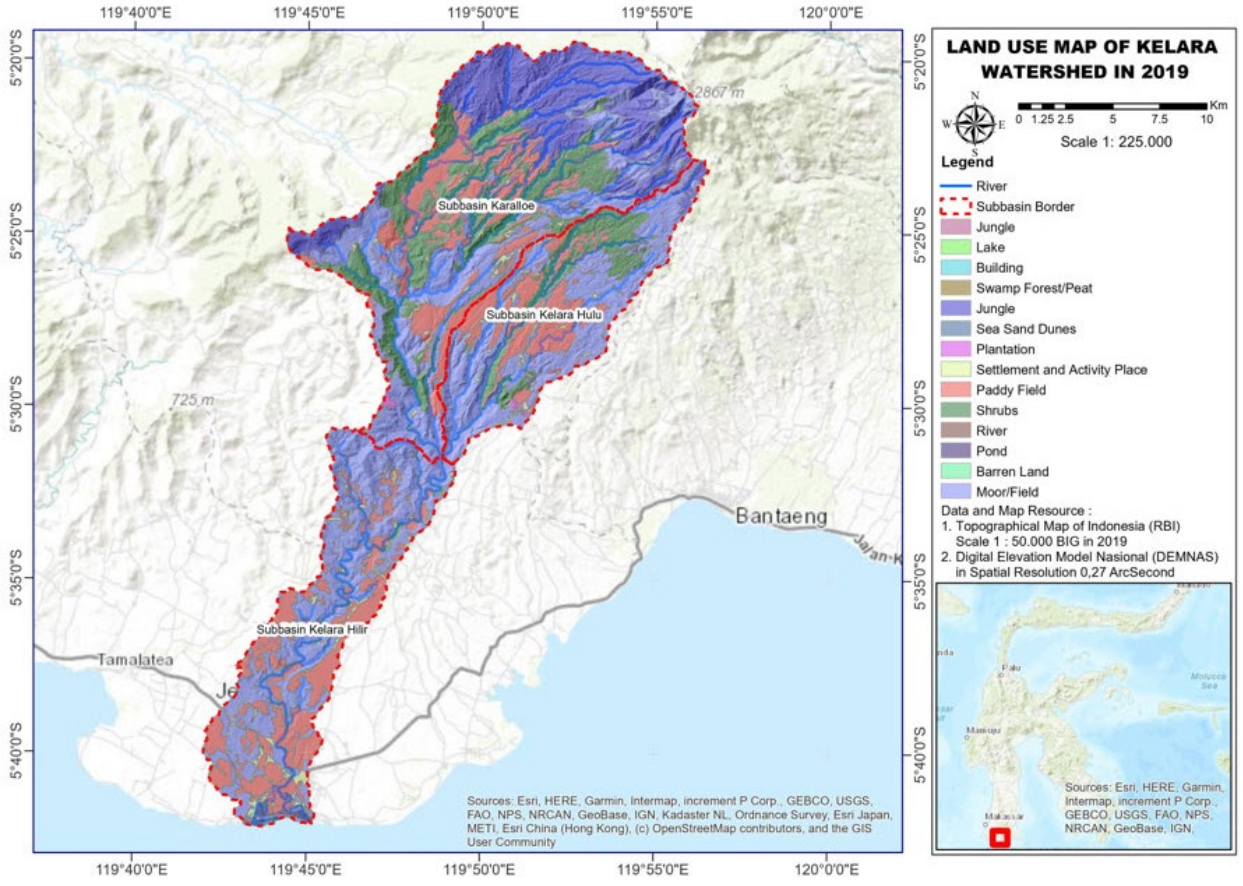

Figure 8 Topographic maps, maps of soil types, and maps of land use patterns in the Kelara watershed.

Figure 8 shows that the Kelara watershed has an area of 386.77 km^2, the length of the main river is 78.4 km, the highest elevation is +848 m.a.s.l., the lowest elevation is +0 m.a.s.l., the average river slope is 0.026%, the soil type is dominated by Dystropepts and the pattern land use is dominated by fields/fields. Based on the analysis of the watershed characteristics, the input parameters in the HEC-HMS application are obtained, which can be seen in Table 1.

Table 1 Parameters of HEC-HMS input materials.

No.	Physical Parameters	Subwatershed		
		Karalloe	Kelara Hulu	Kelara Hilir
1	Watershed area (km^2)	195.23	86.89	104.65
2	Initial Abstraction (mm)	23.40	16.33	20.924
3	Curve Number (CN)	68	76	71
4	Impervious (%)	0.58	0.93	1.59
5	Time Lag (minutes)	124.17	53.89	345.12

For the rainfall data itself, 4 posts are used to represent the upstream, middle stream, and downstream, which can be seen in Figure 9.

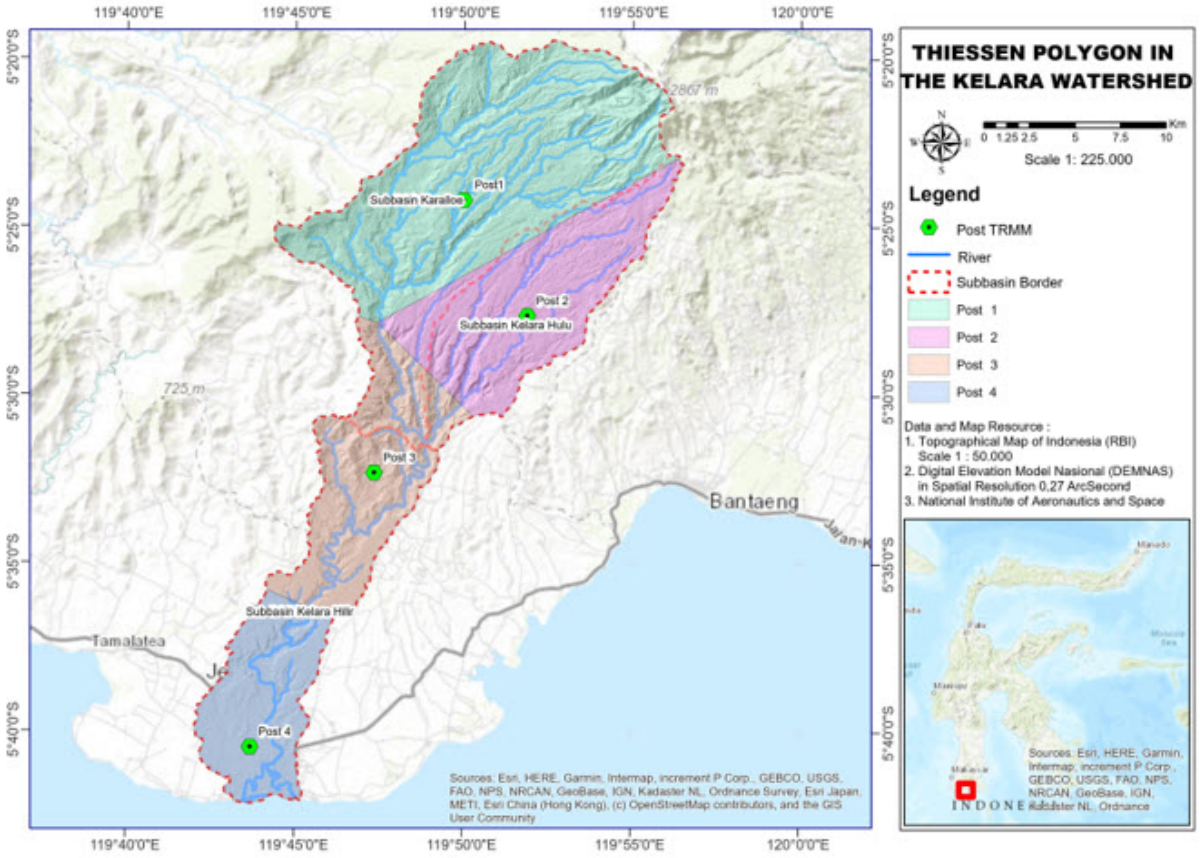

Figure 9 TRMM rain post.

In the hydrological analysis, the maximum rainfall used is the highest in one day, at each rain post, for one month, for each year, with the results of data recapitulation, which can be seen in Table 2.

Table 2 Annual maximum daily rainfall in the Kelara Watershed.

Year	Maximum Daily Rainfall (mm)			
	Post 1	Post 2	Post 3	Post 4
1998	87	64	80	117
1999	128	137	173	210
2000	108	112	96	126
2001	95	99	98	131
2002	75	75	83	88
2003	96	87	88	103
2004	102	103	96	88
2005	85	71	77	76
2006	129	123	97	120
2007	73	79	72	100
2008	72	72	96	91
2009	84	89	80	88
2010	111	134	101	93
2011	84	87	94	117
2012	70	73	81	101
2013	108	118	155	212
2014	74	79	96	100
2015	116	113	138	151
2016	80	82	101	101
2017	95	100	102	144
2018	80	76	78	92
2019	109	127	138	149
2020	89	100	74	84

Parameter data in Table 1 and rainfall data obtained are then input into the HEC–HMS software to determine the amount of flood discharge from the Kelara watershed. The Kelara watershed flood hydrograph analysis results can be seen in Figure 10.

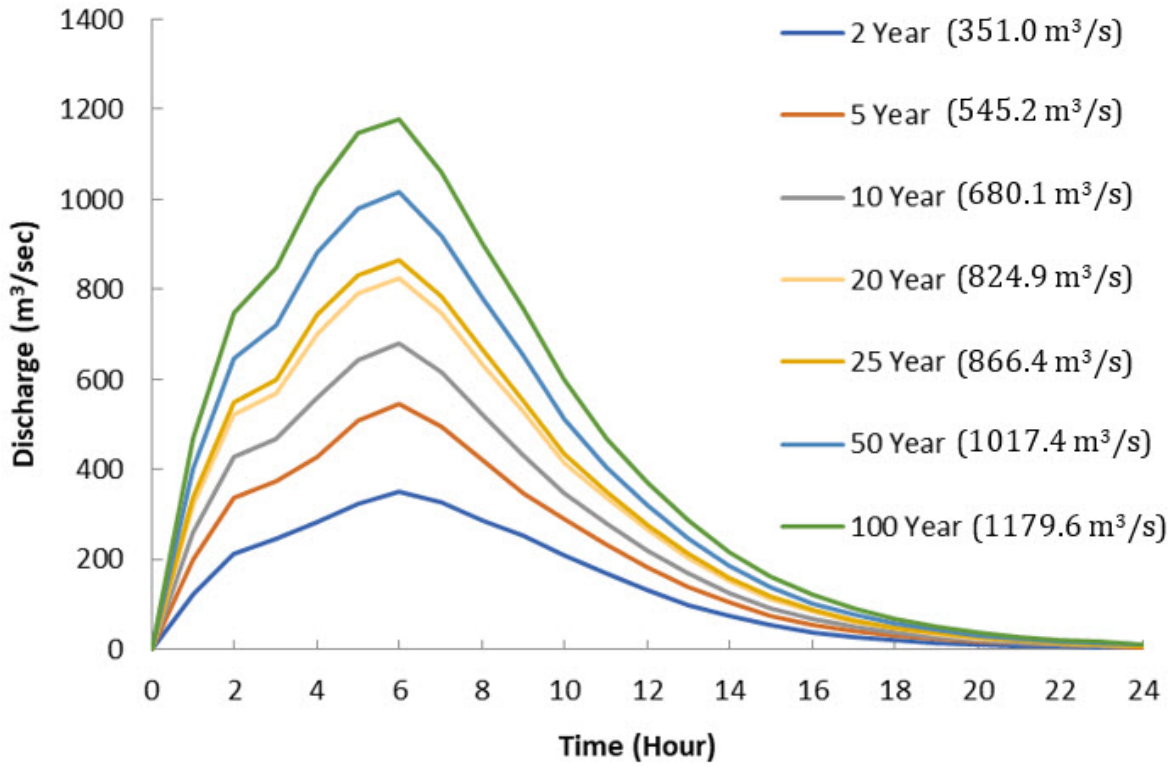

Figure 10 Kelara Watershed flood hydrograph.

Figure 10 shows the results of the hydrological analysis of the HSS SCS method with Q2 max of 351 m^3/s, Q5 max of 545.2 m^3/s, Q10 max of 680.1 m^3/s, Q20 max of 824.9 m^3/s, Q25 max of 866.4 m^3/s, Q50 max of 1017.4 m^3/s and Q100 max of 1179.6 m^3/s. The flood discharge data will be used in a 2D HEC-RAS flood simulation to determine the distribution of floods due to the overflow of the Kelara River.

3.2 2D Numerical Simulation

2D Simulation model validation

Before carrying out a flood inundation simulation based on the design flood discharge, it is necessary to validate the 2D simulation model that has been compiled with the results of instantaneous flow velocity measurements in the field. Measurement of flood flow velocity is carried out using the monitoring method and utilizing a current meter (SNI 8066: 2015). The discharge and current velocity data from field measurements can be seen in Table 3.

Table 3 Flow data and measurement of the Kelara River.

No.	Location	Coordinate	Average Current Speed (m/s)	Discharge (m^3/s)	Description
1	Point 1	5°36'19.75"LS & 119°45'20.23"E	0.358140	7.532864	Simulation Input Point (Inflow)
2	Point 2	5°38'37.37"LS & 119°44'8.43"E	0.124969	7.810377	Simulation Validation Point
3	Point 3	5°39'47.31"LS & 119°44'8.66"E	0.246124	34.03387	Simulation Validation Point
4	Point 4	5°40'44.31"LS & 119°44'34.97"E	0.411389	48.62094	Simulation Validation Point

The measurement data at point 1 is used as an inflow point, while points 2–4 are used as validation points for 2D simulations.

Figure 11 shows a comparison of the current velocity of the simulation results, and the measurement results that were used as validation.

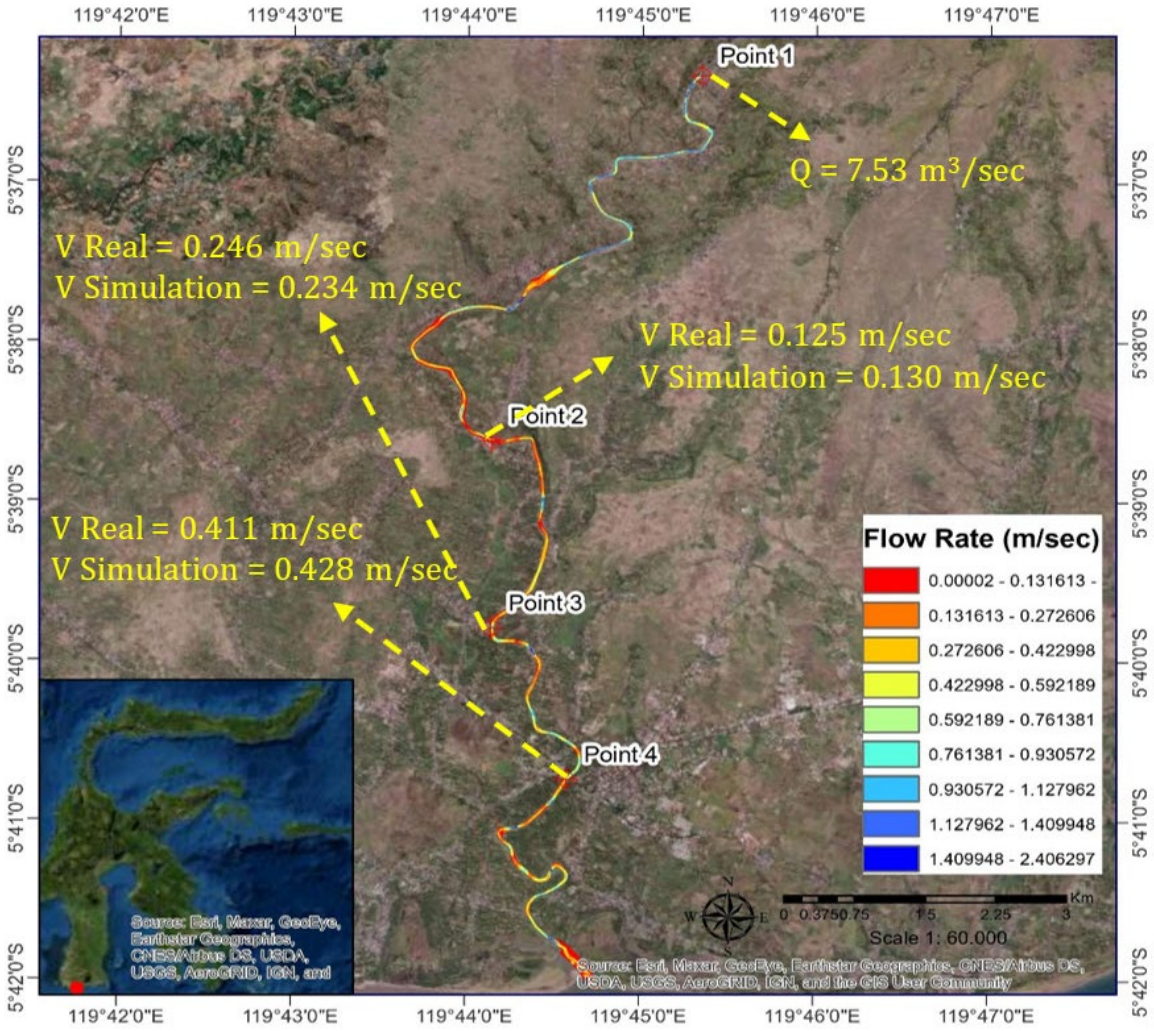

Figure 11 Comparison of simulation results of flow velocity and Kelara River field measurement.

Validation of the 2D simulation model was carried out at points 2, 3, and 4, where, based on the results of current measurements in the field, the average flow velocity at each point was 0.125 m/s, 0.246 m/s, and 0.411 m/s, while the simulation results obtained flow velocities of 0.130 m/s, 0.234 m/s, and 0.428 m/s. By using the Mean Absolute Percentage Error (MAPE) approach, the percentage error value between the field current velocity data and the simulated current velocity data is 4.4%. Based on the interpretation of the MAPE approach, with a value of <10%, the simulation model capability is categorized as very good.

Flood inundation simulation

Inundation simulation using the HEC-RAS application aims to describe flood propagation events, especially in the flood event on January 22, 2019 which was the worst flood that occurred on the Kelara River. To find out the return period of the flood that occurred on January 22, 2019, it is necessary to simulate the return period of Q2–Q100, then verify the simulation results and flood heights in the field using the trial and error method. The comparison of flood depth data from simulation results and historical flooding can be seen in Figure 12.

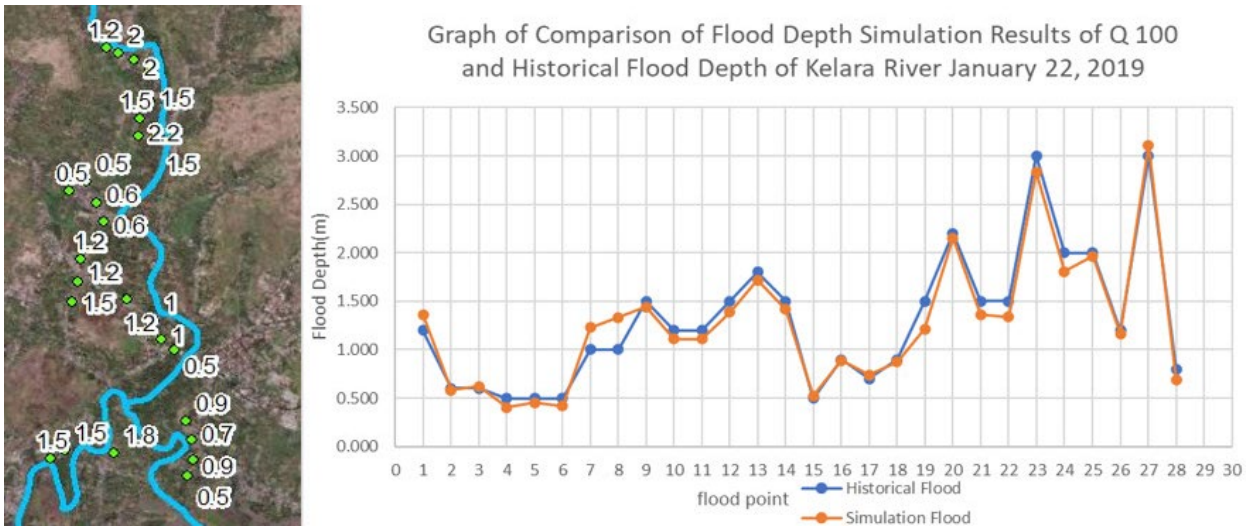

Figure 12 Comparison of maximum simulation flood depth and historical flood depth.

Based on the Mean Absolute Percentage Error (MAPE) approach, the percentage error value between the flood data from the Q100 simulation and the historical flood on 22 January 2019, is 8.208%. Based on the interpretation of the MAPE approach, with a value of <10%, the ability of the simulation model is satisfying (Khair et al. 2017). The simulation results show that the flood that occurred on January 22, 2019 was a 100-year anniversary flood.

Furthermore, simulation results are classified into 3 classes, namely a depth of < 0.76 m is a low hazard class, a depth of 0.76-1.5 m is a moderate hazard class, and a depth of > 1.5 m is a high hazard class [25] which shown in Figure 13.

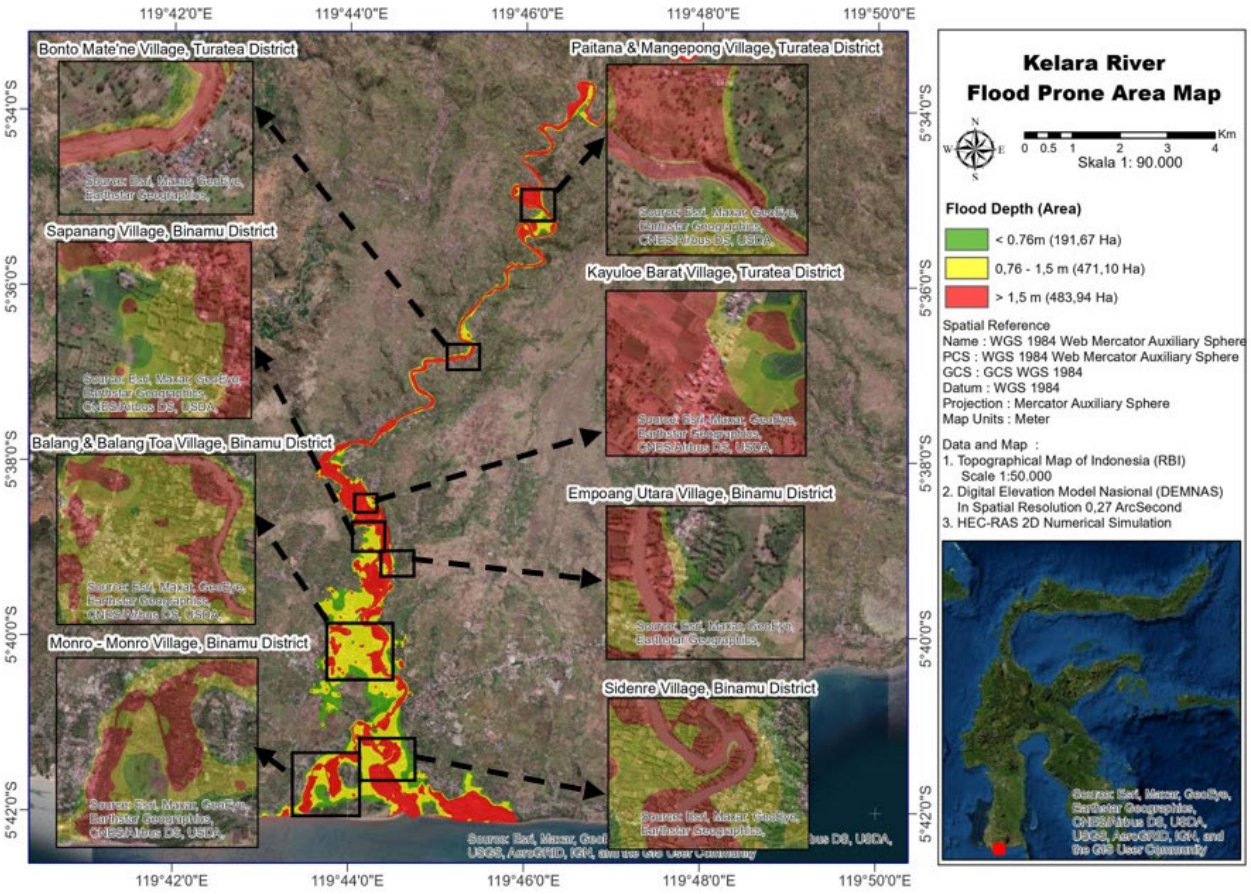

Figure 13 Map of the Kelara River flood-prone area.

Figure 13 shows that there are 10 points of residential areas that must be alerted during high rainfall intensity, which are Paitana Village, Mangepong Village, Bonto Ma'tene Village, Kayuloe Barat Village, Sapanang Village, Empoang Utara Village, Balang Village, Balang Toa Village, Sindre Village, and Monro-Monro Village.

3.3 Kelara River Flood Early Warning System

One of the mitigations to solve the Kelara River flooding is to create a flood early warning system, so that the communities/areas that are included in flood-prone areas can anticipate the flood beforehand using flood information at the upstream lookout point. The location of lookout points on the Kelara River can be seen in Table 4.

Table 4 Flood warning lookout point location data.

No.	Code	Coordinate	Location
1	Lookout Point 1 (Upstream)	5°34'6.15"LS & 119°46'43.11"E	Paitana Village, District Turatea
2	Lookout Point 2	5°34'51.75" LS & 119°46'4.29" E	Paitana Village, District Turatea
3	Lookout Point 3	5°35'14.22"LS & 119°46'17.75"E	Mangepong Village, Kec. Turatea
4	Lookout Point 4	5°36'17.76"LS & 119°45'21.65"E	Bonto Matene Village, District Turatea
5	Lookout Point 5	5°38'33.52"LS & 119°44'0.77"E	Kayuloe Barat Village, Kec. Turatea
6	Lookout Point 6	5°38'40.23"LS & 119°44'23.08"E	Sapanag Village, District Binamu
7	Lookout Point 7	5°40'12.37"LS & 119°44'21.42"E	Balang Village, Kec. Binamu
8	Lookout Point 8	5°41'28.63"LS & 119°44'24.38"E	Sidenre Village, Kec. Binamu
9	Lookout Point 9	5°41'23.38"LS & 119°44'3.96"E	Monro – Monro Village, Kec. Binamu
10	Lookout Point 10	5°41'27.82"LS & 119°43'51.82"E	Monro – Monro Village, Kec. Binamu

Flood forecasting analysis

The basic concept of the flood forecasting program to be developed is to determine the flood travel time and three critical times for each lookout point based on the flood alert level. To facilitate flood forecasting, it is necessary to know the intensity of rain that occurs in the three sub-watersheds with several return periods of flooding. The rain intensity from the Mononobe analysis shows that if the rain intensity is > 50.36 mm/hour from the three sub-watersheds, it is necessary to be aware of a potential flood disaster.

Flood time travel

Time travel is the time it takes for the flood to flow from the upstream lookout point to the next lookout point. The purpose of this system is to determine the flood travel time from the upstream lookout point to the next lookout point in the hope that after receiving information from the upstream community, the downstream community can respond to the information quickly and accurately. Preparedness and reaction speed are required due to critical conditions and limited mitigation time. Time travel for each lookout point based on the simulation results can be seen in Table 5 and Figure 14.

Table 5 Time travel lookout point FEWS Kelara River.

No.	Lookout Point	Distance from Lookout Point to Previous Point (km)	Time Travel (minute)
1	LP.1/TP.Hulu	0	0
2	LP.2	4.85	37
3	LP.3	6.46	49
4	LP.4	10.87	73
5	LP.5	18.4	119
6	LP.6	19.21	128
7	LP.7	22.64	167
8	LP.8	26.59	206
9	LP.9	29.99	248
10	LP.10	30.46	261

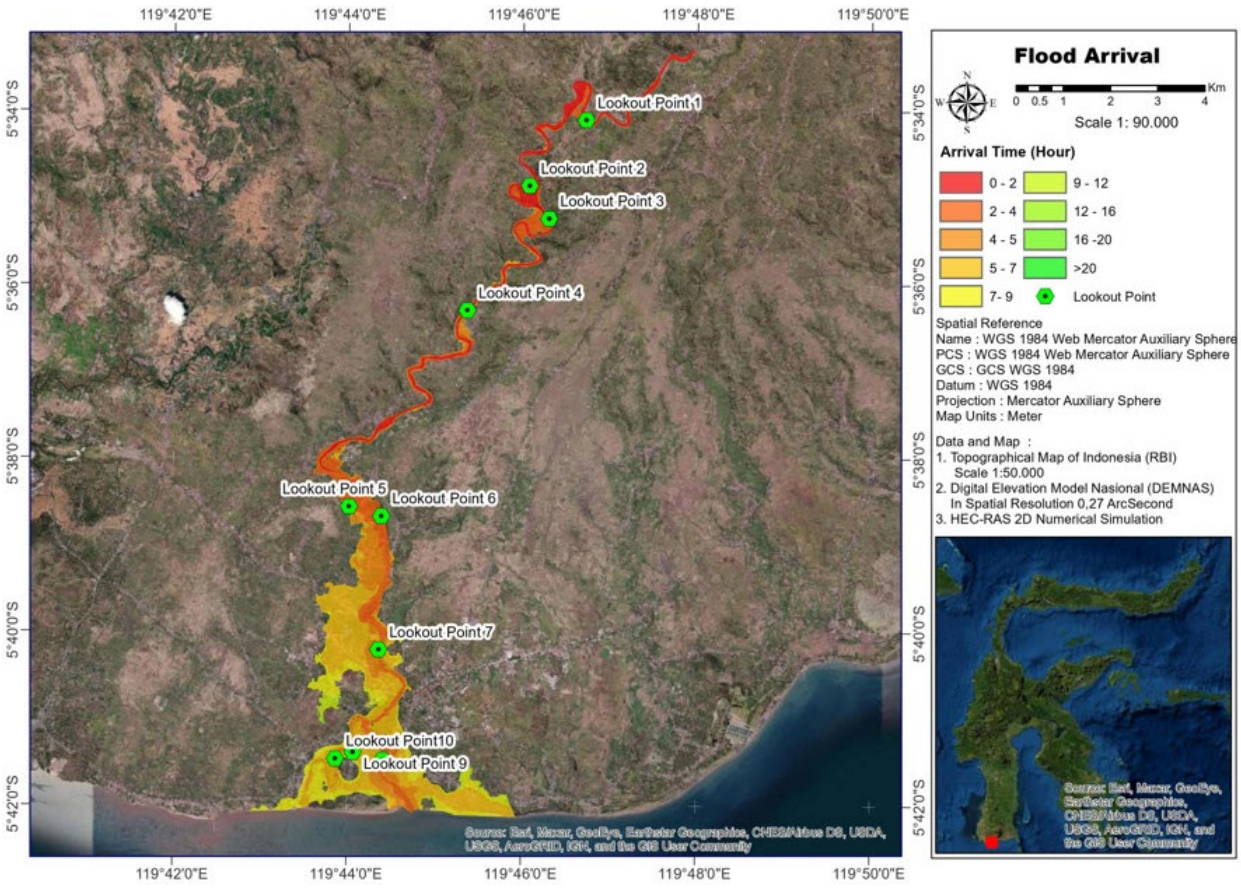

Figure 14 Flood arrival time map.

Lookout point critical time forecast

The purpose of this stage is to estimate the time it takes for the flood water level to go to green alert, yellow alert, and red alert based on the simulation results, and determine the standby limit according to the height of the guard at the lookout point. The results of forecasting the critical time of the lookout point based on the simulation results can be seen in Figure 15.

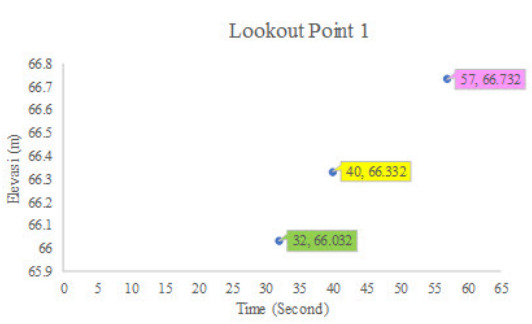
Lookout Point 1
Elevasi (m)
Time (Second)
57, 66.732
40, 66.332
32, 66.032

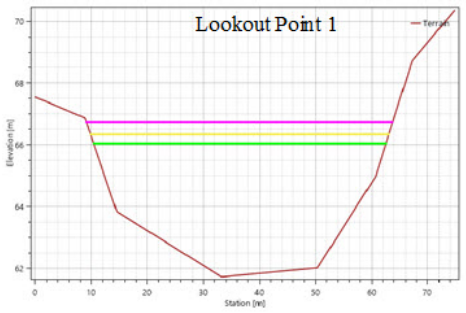
Lookout Point 1
Terrain
Elevation [m]
Station [m]

(a)

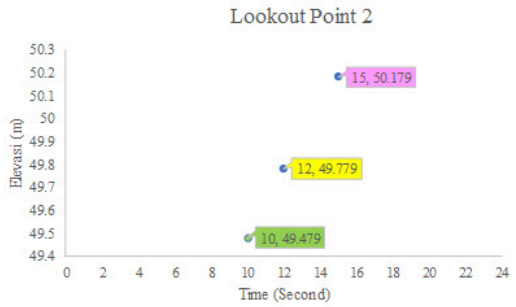
Lookout Point 2
Elevasi (m)
Time (Second)
15, 50.179
12, 49.779
10, 49.479

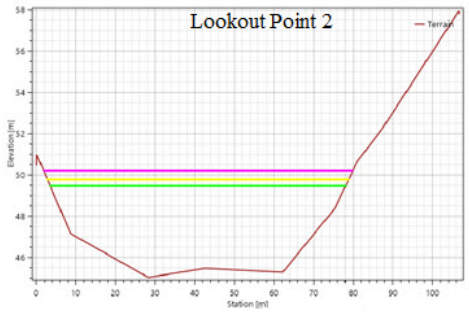
Lookout Point 2
Terrain
Elevation [m]
Station [m]

(b)

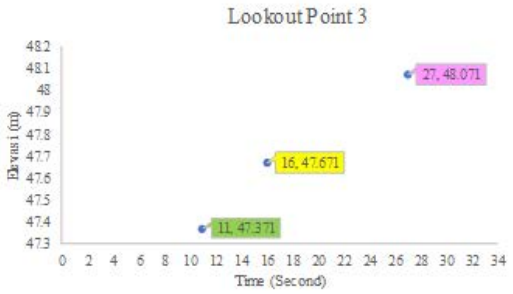
Lookout Point 3
Elevasi (m)
Time (Second)
27, 48.071
16, 47.671
11, 47.371

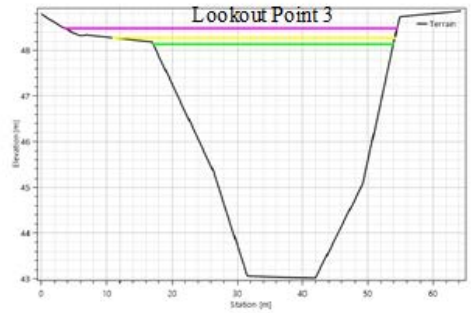
Lookout Point 3
Terrain
Elevation [m]
Station [m]

(c)

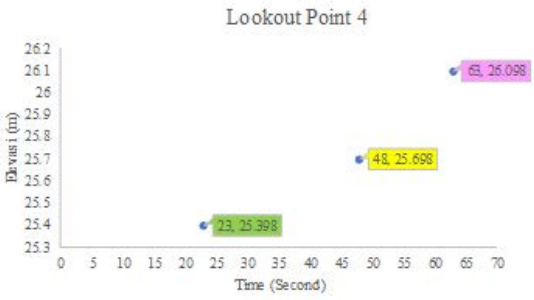
Lookout Point 4
Elevasi (m)
Time (Second)
63, 26.098
48, 25.698
23, 25.398

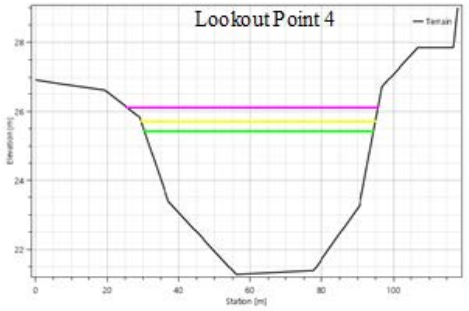
Lookout Point 4
Terrain
Elevation [m]
Station [m]

(d)

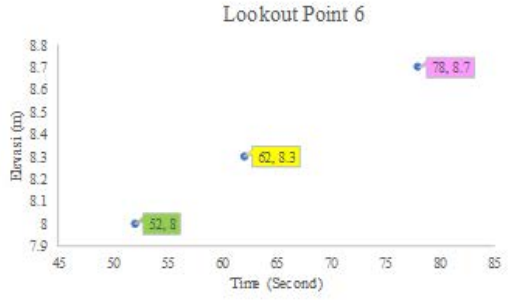
Lookout Point 6
Elevasi (m)
Time (Second)
78, 8.7
62, 8.3
52, 8

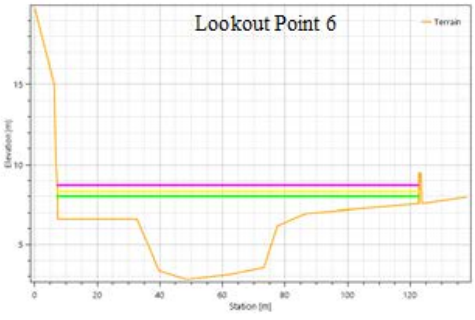
Lookout Point 6
Terrain
Elevation [m]
Station [m]

(e)

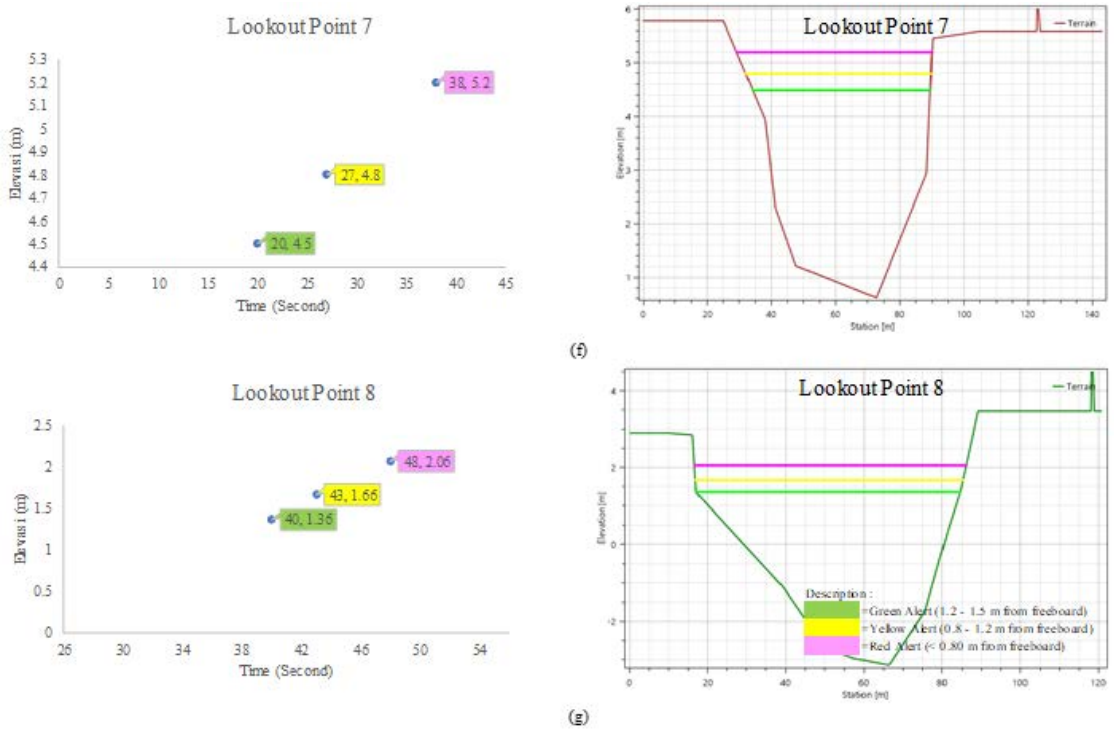

Figure 15 Critical time forecasting for lookout points.

Figure 15 shows how the estimated critical time forecast for the lookout point is obtained, namely the time required for flooding from normal conditions to red alerts. Where green alerts the time to prepare and get ready, yellow alerts the time for evacuation preparation, and a red alert is the time for evacuation.

At Lookout Point 1 (Figure 15a), the time required from normal to green alert at an elevation of +66.032 m is 32 minutes, green alert to yellow alert at an elevation of + 66.332 m is 8 minutes, and yellow alert to red alert at elevation + 66.732 m is 17 minutes. The total time required from normal to red alert conditions is 57 minutes.

At Lookout Point 2 (Figure 15b), the time required from normal to green alert at an elevation of +49.479 m is 10 minutes, green alert to yellow alert at an elevation of + 49.779 m is 2 minutes, and yellow alert to red alert at elevation + 50.179 m is 3 minutes. The total time required from normal to red alert conditions is 15 minutes.

At Lookout Point 3 (Figure 15c), the time required from normal to green alert at an elevation of +43.371 m is 11 minutes, green alert to yellow alert at an elevation of + 47.671 m is 5 minutes, and yellow alert to red alert at elevation + 48.071 m is 11 minutes. The total time required from normal to red alert conditions is 27 minutes.

At Lookout Point 4 (Figure 15d), the time required from normal to green alert at an elevation of +25.398 m is 23 minutes, green alert to yellow alert at an elevation of + 25.698 m is 25 minutes, and yellow alert to red alert at elevation + 26.098 m is 15 minutes. The total time required from normal to red alert is 1 hour 3 minutes.

At Lookout Point 6 (Figure 15e), the time required from normal to green alert at +8 m elevation is 52 minutes, green alert to yellow alert at +8.3 m elevation is 10 minutes, and yellow alert to

red alert at +8.7 m elevation is 16 minutes. The total time required from normal to red alert is 1 hour 18 minutes.

At Lookout Point 7 (Figure 15f), the time required from normal to green alert at an elevation of +4.5 m is 20 minutes, green alert to yellow alert at an elevation of + 4.8 m is 7 minutes, and yellow alert to red alert at +5.2 m elevation is 11 minutes. The total time required from normal to red alert conditions is 38 minutes.

At Lookout Point 8 (Figure 15g), the time required from normal to green alert at an elevation of +1.36 m is 40 minutes, green alert to yellow alert at an elevation of +1.66 m is 3 minutes, and yellow alert to red alert at elevation + 2.06 m is 5 minutes. The total time required from normal to red alert conditions is 48 minutes.

At Lookout Points 5, 9, and 10, the time required for normal to standby conditions is very small, so the standby time at these lookout points is only based on time travel from the upstream lookout point (TP.1).

Based on the results of the analysis of time travel and the time left at the lookout points, the total time required from the upstream lookout point to the standby condition at each lookout point can be seen in Table 6.

Table 6 Flood alert time at lookout points.

Lookout Point	Total Time
LP.1/Hulu	57 Minutes
LP.2	52 Minutes
LP.3	1 Hour 16 Minutes
LP.4	2 Hours 16 Minutes
LP.5	1 Hour 59 Minutes
LP.6	3 Hours 26 Minutes
LP.7	3 Hours 25 Minutes
LP.8	4 Hours 14 Minutes
LP.9	4 Hours 8 Minutes
LP.10	4 Hours 21 Minutes

Table 6 shows the arrival time of flooding to residential areas according to distance and topographic conditions. The fastest red alert time is at Lookout Point 2, located in Paitana Village, within 52 minutes, while the longest time is at Lookout Point 10, located in Monro-Monro Village, within 4 hours and 21 minutes.

These results need to be communicated to people living in flood-prone areas to be alert when the intensity of rain is high, so as to reduce the impact/loss associated with flood disasters. Furthermore, for policy makers and authorized agencies, the proposed application of sensors at monitoring points should be one of the mitigation proposals with a flood early warning system so that the community can know the time needed to evacuate to a safer place in the event of a disaster.

4. CONCLUSION

In this study, flood propagation was analyzed using 2D numerical simulations to see the distribution of floods along the Kelara River channel as a reference in the preparation of a flood-prone area model that was urgently needed by the Jeneponto Regency Government in supporting infrastructure planning, transportation facilities, and other planning, including planning an area by developers to determine insurance and flood insurance for buildings, houses, offices, and so on, and provide an assessment of the time of flood propagation as a flood early warning system to anticipate the time and occurrence of disasters.

However, related to numerical modeling, one of the problems that is often encountered is that high-resolution models have a very long computational time at a high cost to predict the time of flood spread, which is needed in the preparation of a flood early warning system. So, this research uses 2D HEC-RAS software with unsteady flow type and Diffusion Wave equation so that the simulation can run stably to overcome these problems. Furthermore, the limitation of this study is that it only uses DEMNAS data with a spatial resolution of 8.4 meters, combined with the results of river topography measurements to run a 2D simulation model. Despite these limitations, such a model can be applied anywhere, provided there is historical flood data to verify the simulation results. This is evidenced by the Mean Absolute Percentage Error (MAPE) approach, where the value of the percentage error between flood data from the simulation is <10%, so the ability of the simulation model can be said to be very good and feasible.

Currently, the most feasible thing to do to improve the accuracy of the simulation in the future is to use drones to capture topographic data which is then combined with bathymetry measurements of riverbeds with the same reference point.

Finally, by looking at the results of this study, we can recommend that the use of numerical simulation of flood propagation HEC-RAS 2D is ideal for use in the preparation of flood-prone areas and flood early warning systems. This simulation must also be equipped with historical flood data to verify the simulation results, because not all natural parameters can be entered into the model so that errors or discrepancies appear in the field.

ACKNOWLEDGMENT

The author would like to express gratitude to the Hydraulics Laboratory of Hasanuddin University and the anonymous reviewers for their constructive suggestions.

REFERENCES

Bagheri, K., W. Requieron, and H. Tavakol. 2020. “A Comparative Study of 2-Dimensional Hydraulic Modeling Software, Case Study: Sorrento Valley, San Diego, California.” *Journal of Water Management Modeling* 28, C471. https://doi.org/10.14796/JWMM.C471

Bakri, B., K. Adam, and A. Rahim. 2021. “Spatio-Temporal Model of Extreme Rainfall Data in the Province of South Sulawesi for a Flood Early Warning System.” *Geomatics and Environmental Engineering* 15 (2): 5–15. https://doi.org/10.7494/geom.2021.15.2.5

Brunner, G.W. 2016. “HEC-RAS, River Analysis System 2D Modeling User’s Manual Version 5.0.” California: Hydrologic Engineering Center, Institute for Water Resources, US Army Corps of Engineers. https://www.hec.usace.army.mil/software/hec-ras/documentation/HEC-RAS 5.0 2D Modeling Users Manual.pdf

Contreras, M.T., J. Gironás, J. Westerink, and C. Escauriaza. 2018. “Advanced Numerical Models for the Propagation of Floods with High-Sediment Concentrations in Mountain Rivers.” Edited by A. Paquier and N. Rivière. E3S Web of Conferences 40 (September): 1–8. https://doi.org/10.1051/e3sconf/20184006039

“Daftar Informasi Bencana Indonesia (DIBI).” 2021. Badan Nasional Penanggulangan Bencana. https://dibi.bnpb.go.id

Di Baldassare, G., A. Castellarin, and A. Brath. 2009. “Analysis of The Effects of Levee Heightening on Flood Propagation: Example of The River Po, Italy.” *Hydrological Sciences Journal* 54 (6): 1007–17. https://doi.org/10.1623/hysj.54.6.1007

Hallegatte, S., C. Green, R.J. Nicholls, and J. Corfee-Morlot. 2013. “Future Flood Losses in Major Coastal Cities.” *Nature Climate Change* 3 (9): 802–6. https://doi.org/10.1038/nclimate1979

Hou, J., H. Han, Z. Li, K. Guo, and Y. Qin. 2018. “Effects of Morphological Change on Fluvial Flood Patterns Evaluated by a Hydro-Geomorphological Model.” *Journal of Hydroinformatics* 20 (3): 633–44. https://doi.org/10.2166/hydro.2018.142

Hou, J., B. Li, Y. Tong, L. Ma, J. Ball, H. Luo, Q. Liang, and J. Xia. 2020. “Cause Analysis for a New Type of Devastating Flash Flood.” *Hydrology Research* 51 (1): 1–16. https://doi.org/10.2166/nh.2019.091

Hou, J., X. Li, G. Bai, X. Wang, Z. Zhang, L. Yang, Y. Du, Y. Ma, D. Fu, and X. Zhang. 2021. “A Deep Learning Technique Based Flood Propagation Experiment.” *Journal of Flood Risk Management* 14 (3): 1–13. https://doi.org/10.1111/jfr3.12718

Karamma, R., and M.S. Pallu. 2018. “Comparison of Model Hidrograf Synthetic Units (HSS) with the Model of Hidrograf Observations on DAS Jeneberang Gowa Regency, Indonesia.” *International Journal of Innovative Science and Research Technology* 3 (2): 617–23.

Khair, U., H. Fahmi, S. Al Hakim, and R. Rahim. 2017. “Forecasting Error Calculation with Mean Absolute Deviation and Mean Absolute Percentage Error.” *Journal of Physics: Conference Series,* 930 012002. https://doi.org/10.1088/1742-6596/930/1/012002

Krzhizhanovskaya, V.V., G.S. Shirshov, N.B. Melnikova, R.G. Belleman, F.I. Rusadi, B.J. Broekhuijsen, B.P. Gouldby, et al. 2011. “Flood Early Warning System: Design, Implementation and Computational Modules.” *Procedia Computer Science* 4: 106–15. https://doi.org/10.1016/j.procs.2011.04.012

Liang, Q. 2010. “Flood Simulation Using a Well-Balanced Shallow Flow Model.” *Journal of Hydraulic Engineering* 136 (9): 669–75. https://doi.org/10.1061/(ASCE)HY.1943-7900.0000219

Lopa, R.T., M.S. Pallu, F. Maricar, B. Bakri, M.F. Maricar, and M.A. Sudarmin. 2018. “Penentuan Kapasitas Pelimpah Bendung Way Yori.” Prosiding Seminar Ilmiah Nasional Sains Dan Teknologi Ke-4 Tahun 2018 4: 501–5.

Merz, B., H. Kreibich, R. Schwarze, and A. Thieken. 2010. “Review Article ‘Assessment of

Economic Flood Damage.'" *Natural Hazards and Earth System Sciences* 10 (8): 1697–1724. https://doi.org/10.5194/nhess-10-1697-2010

Modul Pengendalian Daya Rusak Air. 2017. Bandung: Kementerian Pekerjaan Umum Dan Perumahan Rakyar Badan Pengembangan Sumber Daya Manusia.

Mujumdar, P.P. 2001. "Flood Wave Propagation." Resonance 6 (5): 66–73. https://doi.org/10.1007/BF02839085

Mustamin, M.R., F. Maricar, and R. Karamma. 2021. "Hydrological Analysis in Selecting Flood Discharge Method in Watershed of Kelara River." *INTEK: Jurnal Penelitian* 8 (2): 141. https://doi.org/10.31963/intek.v8i2.2874

Praveen, S.S., V.S. Babu, A. Vijayan, and S. Babu S. 2020. "Numerical Modelling of Flood Inundation and Run-Up along the Banks of Pamba River, South West Coast of India." *Journal of Advanced Research in Alternative Energy, Environment and Ecology* 07 (01): 8–14. https://www.thejournalshouse.com/index.php/AltEnergy-Ecology-EnvironmentJ/article/view/135

Rak, G., D. Kozelj, and F. Steinman. 2016. "The Impact of Floodplain Land Use on Flood Wave Propagation." Natural Hazards 83 (1): 425–43. https://doi.org/10.1007/s11069-016-2322-0

Riswal, K., and A.S. Sukri. 2020. "Kajian Koefisien Aliran Terhadap Perubahan Debit Banjir Pada DAS Karalloe Dengan Aplikasi ArcGIS." *SemanTIK* 6 (1): 1–8. https://doi.org/10.5281/zenodo.3818243

Romali, N.S. 2018. "Application of HEC-RAS and Arc GIS for Floodplain Mapping in Segamat Town, Malaysia." *International Journal of GEOMATE* 14 (43). https://doi.org/10.21660/2018.43.3656

Samsuar, S., and M.T. Sapsal. 2018. "Analisis Ketersediaan Air Pada DAS Kelara Dalam Mendukung Program Percetakan Sawah Baru Di Kabupaten Jeneponto." *Jurnal Agritechno*, April, 26–34. https://doi.org/10.20956/at.v11i1.84

Satriani, S., R. Lopa, and F. Maricar. 2021. "Storage Capacity Analysis of Nipa Nipa Regulation Pond Using Ripple Method." IOP Conference Series: Materials Science and Engineering 1098 (2): 022054. https://doi.org/10.1088/1757-899X/1098/2/022054

Son, K-I., and W. Jeong. 2019. "Numerical Simulation of Flood Inundation in a Small-Scale Coastal Urban Area Due to Intense Rainfall and Poor Inner Drainage." *Water* 11 (11): 1–21. https://doi.org/10.3390/w11112269

Sudarmin, M.A., F. Maricar, and R.T. Lopa. 2022. "Realtime Flood Propagation on the Downstream of Bili-Bili Reservoir With Hydraulic Routing." In *AIP Conference Proceedings* 2453, 020025. https://doi.org/10.1063/5.0095391

Vernimmen, R.R.E., A. Hooijer, Mamenun, E. Aldrian, and A.I.J.M. van Dijk. 2012. "Evaluation and Bias Correction of Satellite Rainfall Data For Drought Monitoring in Indonesia." *Hydrology and Earth System Sciences* 16 (1): 133–46. https://doi.org/10.5194/hess-16-133-2012

Vijayan, A., S.S. Praveen, V.S. Babu, and S. Babu S. 2021. "Simulation Studies of Flood Along the Periyar River Basin, Central Kerala, India." *Journal of Advanced Research in Geo Sciences & Remote Sensing* 8 (2): 1–7.

Wijayanti, P., X. Zhu, P. Hellegers, Y. Budiyono, and E.C. van Ierland. 2017. "Estimation of River Flood Damages in Jakarta, Indonesia." *Natural Hazards* 86 (3): 1059–79. https://doi.org/10.1007/s11069-016-2730-1

Xia, X., Q. Liang, X. Ming, and J. Hou. 2017. “An Efficient and Stable Hydrodynamic Model With Novel Source Term Discretization Schemes For Overland Flow and Flood Simulations.” *Water Resources Research 53* (5): 3730–59. https://doi.org/10.1002/2016WR020055

Yang, Q., T. Liu, J. Zhai, and X. Wang. 2021. “Numerical Investigation of a Flash Flood Process That Occurred in Zhongdu River, Sichuan, China.” *Frontiers in Earth Science* 9 (July): 1–11. https://doi.org/10.3389/feart.2021.686925